

<https://doi.org/10.15407/ujpe65.12.1089>

M. DUFANETS, V. SKLYARCHUK, YU. PLEVACHUK

Ivan Franko National University of L'viv
(8, Kyrylo i Mefodiy Str., Lviv 79005, Ukraine)

STRUCTURE-SENSITIVE PROPERTIES OF CU-BASED BINARY SUBSYSTEMS OF HIGH-ENTROPY Bi–Cu–Ga–Sn–Pb ALLOY

The temperature dependences of the viscosity, electrical conductivity, and thermal emf of the binary melts $Cu_{50}Bi_{50}$, $Cu_{50}Ga_{50}$, $Cu_{50}Pb_{50}$, and $Cu_{50}Sn_{50}$ with equiatomic concentrations, which are components of the high-entropy Bi–Cu–Ga–Sn–Pb alloy, have been studied. Based on the obtained results, the activation energy of the viscous flow and the configurational entropy of mixing are calculated. The obtained negative values of the mixing entropy testify to a structural ordering in the system.

Keywords: high-entropy alloys, viscosity, electrical conductivity, thermal emf.

1. Introduction

High-entropy alloys containing five or more metal elements taken in the equiatomic or near-equiatomic ratio have been intensively studied during recent years. Information obtained from the physical metal science and on the basis of corresponding phase diagrams makes it possible to suppose that such multicomponent alloys can form dozens of phases and intermetallic compounds that are characterized by complicated and fragile microstructures. The analysis and engineering of those alloys are difficult, so they have a limited scope of practical applications. But, on the contrary to such expectations, experimental results testify that the mixing entropy of those alloys, which is higher in comparison with that for traditional alloys ($S_{\text{mix}} > 12 \text{ J mol}^{-1}\text{K}^{-1}$), favors the formation of solid phases with simple structures and, in such a way, counteracts the formation of intermetallic compounds [1–3]. The properties of this kind are of paramount importance for the development and application of indicated alloys. The latter are characterized by the high strength, hardness, wear resistance, exceptional high temperature strength, structural resistance, and resistance to the corrosion and oxidation [4–6].

Because of their properties, high-entropy alloys can be used as coatings for instruments, molds, diffusion barriers, and soft magnetic films. Such advantageous

properties of high-entropy alloys originate from the slow diffusion of atoms in the multicomponent matrix of elements, strong lattice distortion that arises owing to the difference between the atomic radii of the alloy's constituents, and the interaction among the elements in the solid-solution-based phases.

However, multicomponent high-entropy alloys with the equiatomic or near-equiatomic contents have not been studied sufficiently in the cited works. The corresponding investigations mainly concerned the phase composition and the microstructural and morphological features of some chemically different high-entropy alloys. For this purpose, the methods of scanning electron microscopy, X-ray diffraction analysis, and X-ray spectroscopy, as well as measurements of some physical and mechanical properties, were applied. The absence of a common viewpoint concerning the nature of phenomena and physical processes occurring in the examined alloys, the structure of the alloys in the liquid state, the transformation of this structure during the cooling, as well as the mechanisms and the sequences of structural and phase transformations during the crystallization, considerably hinders the development of fundamental ideas about high-entropy alloys and prevents from finding new areas of their practical application. It is worth noting that the processes of atomic solution formation take place just in the liquid state. Therefore, it is at this initial stage of the structure formation when this process can be affected and changed in the required direction in the easiest way.

© M. DUFANETS, V. SKLYARCHUK,
YU. PLEVACHUK, 2020

ISSN 2071-0186. Ukr. J. Phys. 2020. Vol. 65, No. 12

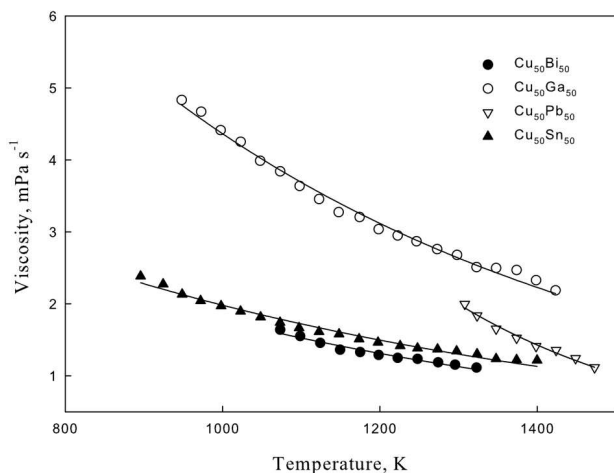


Fig. 1. Temperature dependences of the viscosity for the $\text{Cu}_{50}\text{Bi}_{50}$, $\text{Cu}_{50}\text{Ga}_{50}$, $\text{Cu}_{50}\text{Pb}_{50}$, and $\text{Cu}_{50}\text{Sn}_{50}$ melts

The study of such multicomponent systems is extremely difficult. Hence, information about the properties of their subsystems that contain a smaller number of components and can be regarded as model systems is necessary to continue the research of the alloy parameters and to manufacture such alloys industrially. In this work, the temperature dependences of the viscosity, electrical conductivity, and thermal emf of the binary melts $\text{Cu}_{50}\text{Bi}_{50}$, $\text{Cu}_{50}\text{Ga}_{50}$, $\text{Cu}_{50}\text{Pb}_{50}$, and $\text{Cu}_{50}\text{Sn}_{50}$ with the equiatomic concentrations, which are model subsystems of the five-component high-entropy alloy Bi–Cu–Ga–Sn–Pb, were studied. On the basis of the results obtained, the activation energy of a viscous flow and the configurational entropy of the mixing were calculated.

2. Experimental Part

The temperature dependences of the viscosity of the examined melts, $\eta(T)$, were experimentally studied using a viscometer and following the method of damped torsional oscillations of a cylinder filled with a liquid (the oscillating crucible method) [7]. A graphite crucible with an inner diameter of 14 mm and a height of 30 mm, which was arranged in a steel cylinder, was filled with a melt to study. In order to prevent the possible evaporation of the specimen, the crucible was hermetically covered with a lid and placed into a chamber with an excessive argon pressure. The period and the logarithmic decrement of the oscillation damping were determined with the help of an optical system.

The viscosity measurements were performed in the cooling regime. The viscosity was calculated according to the modified Roscoe equation for cylindrical specimens with an uncovered surface [8]. The measurements were performed in an atmosphere of 90% Ar + 10% H_2 . A uniform temperature field up to 1400 K was maintained in the chamber. The temperature was measured using a WRe-5/20 thermocouple located under the container. The error of viscosity measurements did not exceed 5%.

The electrical conductivity and the thermal emf were measured in the argon atmosphere (a pressure up to 10 MPa) following the 4-point contact method. Measuring cells fabricated from pressed boron nitride in the form of vertical containers 60 mm in height and 3 mm in diameter were applied. The cell design allowed the measurements of the electrical resistance and the thermal emf to be carried out simultaneously. A high-temperature heater with three independently controllable heating elements made it possible to maintain a uniform temperature field (to an accuracy of 0.2–0.3 K) in the working temperature interval when measuring the electrical resistance. It also allowed a temperature difference of up to 15–20 K to be created along the cell when measuring the thermal emf.

The melt components were weighed to an accuracy of 10^{-4} g. The melts were synthesized in evacuated and sealed quartz ampoules at a residual pressure of 10–15 Pa. Then, they were directly introduced into the cells. The temperature measurements were carried out using tungsten-rhenium thermocouples WRe5/20. The thermocouple junction was located in a mass of graphite in order to protect it from the aggressive melt environment. The thermocouple electrodes of the same type were used as potential probes in the electrical conductivity measurements.

The experimental installation and the measurement procedure were described in work [9]. The determination error did not exceed 2% for the electrical conductivity, $\sigma(T)$, and 5% for the thermal emf, $S(T)$.

3. Experimental Results and Their Discussion

In Fig. 1, the temperature dependences of the dynamic viscosity in the binary melts $\text{Cu}_{50}\text{Bi}_{50}$, $\text{Cu}_{50}\text{Ga}_{50}$, $\text{Cu}_{50}\text{Pb}_{50}$, and $\text{Cu}_{50}\text{Sn}_{50}$ are shown. When the melts

are cooled down, their viscosity η increases according to the Arrhenius law

$$\eta_0 = \eta_0 \exp\left(\frac{E}{RT}\right), \quad (1)$$

where η_0 is the viscosity of the ideal liquid (it is a constant or a quantity weakly dependent on the temperature), E the activation energy of a viscous flow, and R the gas constant. Note that the obtained results are in agreement with the data obtained in work [10]. The viscosity dependences $\eta(T)$ are smooth curves and do not reveal any anomalies in the whole temperature interval.

The calculated activation energy of the viscous flow equals 18.5 kJ/mol for $\text{Cu}_{50}\text{Bi}_{50}$, 18.4 kJ/mol for $\text{Cu}_{50}\text{Ga}_{50}$, 45.8 kJ/mol for $\text{Cu}_{50}\text{Pb}_{50}$, and 13.0 kJ/mol for $\text{Cu}_{50}\text{Sn}_{50}$. The maximum value of the dynamic viscosity was found for the melt $\text{Cu}_{50}\text{Ga}_{50}$: it is equal to 5 mPa s in the crystallization region but decreases to 2.5 mPa s at 1400 K. From the experimental results, the preexponential factor η_0 in Eq. (1) was determined (see Table). It allowed us to calculate the configurational entropy of the melt mixing, ΔS , using the formula [10]:

$$\eta_0 = \frac{\hbar N_A}{\mu} \exp\left(-\frac{\Delta S}{R}\right), \quad (2)$$

where \hbar is the Planck constant, N_A the Avogadro number, and μ the molar mass. The obtained negative values of the mixing entropy testify to a structural ordering in the melts.

The experimental temperature dependences of the electrical conductivity and the thermal emf in the researched melts are depicted in Figs. 2 and 3, respectively. The results obtained for the Cu–Pb system agree well with the data of work [11]. The magnitudes of the electrical conductivity vary within an interval of 19000–16000 $\Omega^{-1}\text{cm}^{-1}$ in the $\text{Cu}_{50}\text{Ga}_{50}$ and $\text{Cu}_{50}\text{Sn}_{50}$ melts, and within an interval of 11000–8000 $\Omega^{-1}\text{cm}^{-1}$ in the $\text{Cu}_{50}\text{Bi}_{50}$ and $\text{Cu}_{50}\text{Pb}_{50}$ alloys. Such a substantial difference between the electrical conductivity magnitudes is evidently associated with the influence of the semimetallic component (Pb or Bi). The electrical conductivity of the $\text{Cu}_{50}\text{Bi}_{50}$, $\text{Cu}_{50}\text{Pb}_{50}$, and $\text{Cu}_{50}\text{Sn}_{50}$ alloys decreases linearly in the course of heating within the whole examined temperature interval. The $\text{Cu}_{50}\text{Ga}_{50}$ alloy is an exception: its electrical conductivity increases

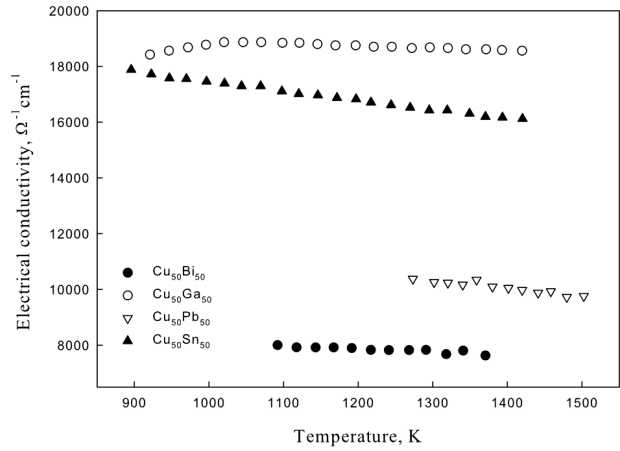


Fig. 2. Temperature dependences of the electrical conductivity for the $\text{Cu}_{50}\text{Bi}_{50}$, $\text{Cu}_{50}\text{Ga}_{50}$, $\text{Cu}_{50}\text{Pb}_{50}$, and $\text{Cu}_{50}\text{Sn}_{50}$ melts

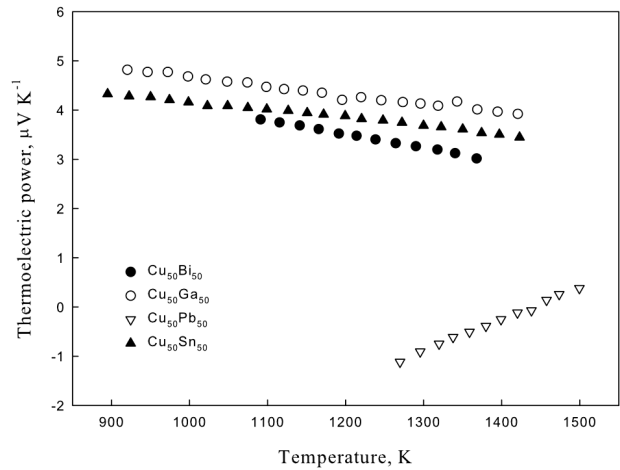


Fig. 3. Temperature dependence of the thermal emf for the $\text{Cu}_{50}\text{Bi}_{50}$, $\text{Cu}_{50}\text{Ga}_{50}$, $\text{Cu}_{50}\text{Pb}_{50}$, and $\text{Cu}_{50}\text{Sn}_{50}$ melts

Approximation parameter values for Eqs. (1) and (2)

Chemical composition	η_0 , mPa s	E , kJ/mol	ΔS , kJ/K
$\text{Cu}_{50}\text{Bi}_{50}$	0.208	18.5	−21.5
$\text{Cu}_{50}\text{Ga}_{50}$	0.488	18.4	−23
$\text{Cu}_{50}\text{Pb}_{50}$	0.029	45.8	−18
$\text{Cu}_{50}\text{Sn}_{50}$	0.411	13.0	−17

with the temperature growth, reaches a maximum near 1100 K, and then monotonically decreases. The thermal emf of the $\text{Cu}_{50}\text{Pb}_{50}$ alloy is negative, and its absolute value decreases from 1.1 to 0.4 $\mu\text{V}/\text{K}$,

as the temperature increases. The thermal electromotive forces of the $\text{Cu}_{50}\text{Bi}_{50}$, $\text{Cu}_{50}\text{Ga}_{50}$, and $\text{Cu}_{50}\text{Sn}_{50}$ alloys are positive within the whole temperature interval and decrease from 4.8 to 3.0 $\mu\text{V}/\text{K}$, as the temperature grows.

The solution of the Boltzmann kinetic equation for electrons in metals expresses a relationship between the thermal emf and the electrical conductivity,

$$S = \frac{\pi^2 k^2 T}{3e} \left(\frac{\partial \ln \sigma(E)}{\partial E} \right)_{E=E_F}. \quad (3)$$

The expression in brackets means that it is necessary first to find the dependence of the electrical conductivity on the energy, and then its energy derivative at the real Fermi energy E_F . From formula (3), it follows that the thermal emf has its own sign. Really, we can write

$$\frac{\partial \ln \sigma(E)}{\partial E} = \frac{\partial \ln \lambda}{\partial E} + \frac{\partial \ln S_F}{\partial E}. \quad (4)$$

So, the energy dependence of the thermal emf is determined by both the electron free path length λ and the Fermi surface area S_F . Moreover, the first term is always positive, whereas the second one can be negative depending on the Fermi surface shape, which really takes place for the $\text{Cu}_{50}\text{Pb}_{50}$ alloy. For all other studied alloys, the thermal emf is positive.

Of particular interest are alloys containing monovalent (copper) and polyvalent (tin, lead, gallium, and others) metals. In the general case, their electrical conductivity is described in the framework of the Faber–Ziman theory. According to it,

$$\sigma = C(k_F) \int_0^{2k_F} |V(k)|^2 |S(k)|^3 dk, \quad (5)$$

where $V(k)$ is the pseudopotential form factor, and $S(k)$ the structure factor. In those alloys, the Fermi wave number increases, if the concentration of the polyvalent metal gradually grows starting from small values. Simultaneously, the value of the structure factor $S(k)$ at $k = 2k_F$ increases. As the temperature grows, the height of the first maximum in the structure factor decreases. At $k = 2k_F$, the reduction of the structure factor value leads to an increase of the electrical conductivity. As a result, there arises an anomalous temperature dependence of the electrical conductivity, which can be observed by the example

of the $\text{Cu}_{50}\text{Ga}_{50}$ alloy. The described effect is possible in other examined alloys as well, but in other concentration intervals.

4. Conclusions

To summarize, information is obtained concerning the temperature dependences of the structure-sensitive properties – viscosity, electrical conductivity, and thermal emf – of the binary $\text{Cu}_{50}\text{Bi}_{50}$, $\text{Cu}_{50}\text{Ga}_{50}$, $\text{Cu}_{50}\text{Pb}_{50}$, and $\text{Cu}_{50}\text{Sn}_{50}$ melts with the corresponding equiatomic concentrations, which are components of the multicomponent Bi–Cu–Ga–Sn–Pb alloy. In particular, the negative values are obtained for the mixing entropy, which testify to the structural ordering in the system. This information is important for studying the characteristics of high-entropy alloys based on those metals, as well as for their industrial manufacture.

This work was sponsored by the Ministry of Education and Science of Ukraine (project No. 0119U002204).

1. J.-W. Yeh, S.-K. Chen, S.-J. Lin, J.-Y. Gan, Ts.-Sh. Chin, T.-Ts. Shun, Ch.-H. Tsau, Sh.-Y. Chang. Nanostructured high-entropy alloys with multiple principal elements: novel alloy design concepts and outcomes. *Adv. Engin. Mater.* **12**, 299 (2004).
2. Y.P. Wang, B.Sh. Li, Zh.F. Heng. Solid solution or intermetallics in a alloy. *Adv. Engin. Mater.* **11**, 641 (2009). high-entropy
3. Yu. Plevachuk, J. Brillo, A. Yakymovych. AlCoCrCuFeNi-based high-entropy alloys: correlation between molar density and enthalpy of mixing in the liquid state. *Metallurg. Mater. Trans. A* **49**, 6544 (2018).
4. O.N. Senkov, G.B. Wilks, J.M. Scott, D.B. Miracle. Mechanical properties of $\text{Nb}_{25}\text{Mo}_{25}\text{Ta}_{25}\text{W}_{25}$ and $\text{V}_{20}\text{Nb}_{20}\text{Mo}_{20}\text{Ta}_{20}\text{W}_{20}$ refractory high entropy alloys. *Intermetallics* **11**, 698 (2011).
5. Y.F. Kao, S.K. Chen, J.H. Sheu, J.T. Lin, W.E. Lin, J.W. Yeh, S.J. Lin, T.H. Liou, C.W. Wang. Hydrogen storage properties of multi-principal-component $\text{CoFeMnTi}_x\text{V}_y\text{Zr}_z$ alloys. *Int. J. Hydrogen Energy* **35**, 9046 (2010).
6. H.-P. Chou, Y.-Sh. Chang, S.-K. Chen, J.-W. Yeh. Microstructure, thermophysical and electrical properties in $\text{Al}_x\text{CoCrFeNi}$ ($0 \leq x \leq 2$) high-entropy alloys. *Mater. Sci. Engin. B* **163**, 184 (2009).
7. S. Mudry, V. Sklyarchuk, and A. Yakymovych. Influence of doping with Ni on viscosity of liquid Al. *J. of Phys. Stud.* **12**, 1601 (2008).

8. S. Mudry, Yu. Plevachuk, V. Sklyarchuk, A. Yakymovych. Viscosity of Bi–Zn liquid alloys. *J. Non-Cryst. Solids* **354**, 4415 (2008).
9. Yu. Plevachuk, V. Sklyarchuk. Electrophysical measurements for strongly aggressive liquid semiconductors. *Meas. Sci. Technol.* **12**, 23 (2001).
10. O.A. Chikova, V.S. Tsepelev, V.V. V'yukhin. Viscosity of high-entropy melts in Cu–Sn–Pb–Bi–Ga, G–Sn, Cu–Pb, Cu–Ga, and Cu–Bi equiatomic compositions. *Russ. J. Non-Ferrous Met.* **56**, 246 (2015).
11. C. Chaib, J-G. Gasser, J. Hugel, L. Roubi. Electrical resistivity and absolute thermoelectric power of liquid copper–lead alloys. *Physica B* **252**, 106 (1998).

Received 23.07.20.

Translated from Ukrainian by O.I. Voitenko

М.В. Дуфанець, В.М. Склярчук, Ю.О. Плевачук

СТРУКТУРНО-ЧУТЛИВІ ВЛАСТИВОСТІ
БІНАРНИХ ПІДСИСТЕМ НА ОСНОВІ Cu
ВИСОКОЕНТРОПІЙНОГО СПЛАВУ Bi–Cu–Ga–Sn–Pb

Резюме

Досліджено температурні залежності в'язкості, електропровідності та термоЕРС бінарних розплавів еквіатомних концентрацій $\text{Cu}_{50}\text{Bi}_{50}$, $\text{Cu}_{50}\text{Ga}_{50}$, $\text{Cu}_{50}\text{Pb}_{50}$, $\text{Cu}_{50}\text{Sn}_{50}$, які є компонентами високоентропійного сплаву Bi–Cu–Ga–Sn–Pb. На основі отриманих результатів розраховано енергію активації в'язкої течії і конфігураційну ентропію змішування. Отримані від'ємні значення ентропії змішування свідчать про структурне впорядкування в системі.